

# Geophysical Research Letters

## RESEARCH LETTER

10.1002/2018GL077524

### Key Points:

- Rainfall excess combined with coastal flooding is a present risk for coastal communities
- This work demonstrates how to define flood transition zones by coupling a coastal inundation model with hydrologic rainfall excess
- The interaction of rainfall excess with coastal surge is nonlinear and is less than the linear superposition of excess and surge

### Supporting Information:

- Supporting Information S1

### Correspondence to:

M. V. Bilskie,  
mbilsk3@lsu.edu

### Citation:

Bilskie, M. V., & Hagen, S. C. (2018). Defining flood zone transitions in low-gradient coastal regions. *Geophysical Research Letters*, 45, 2761–2770. <https://doi.org/10.1002/2018GL077524>

Received 22 NOV 2017

Accepted 12 MAR 2018

Accepted article online 14 MAR 2018

Published online 25 MAR 2018

## Defining Flood Zone Transitions in Low-Gradient Coastal Regions

M. V. Bilskie<sup>1</sup>  and S. C. Hagen<sup>1,2,3</sup> 

<sup>1</sup>Center for Coastal Resiliency, Louisiana State University, Baton Rouge, LA, USA, <sup>2</sup>Department of Civil and Environmental Engineering, Louisiana State University, Baton Rouge, LA, USA, <sup>3</sup>Center for Computation and Technology, Louisiana State University, Baton Rouge, LA, USA

**Abstract** Worldwide, coastal, and deltaic communities are susceptible to flooding from the individual and combined effects of rainfall excess and astronomic tide and storm surge inundation. Such flood events are a present (and future) cause of concern as observed from recent storms such as the 2016 Louisiana flood and Hurricanes Harvey, Irma, and Maria. To assess flood risk across coastal landscapes, it is advantageous to first delineate flood transition zones, which we define as areas susceptible to hydrologic and coastal flooding and their collective interaction. We utilize numerical simulations combining rainfall excess and storm surge for the 2016 Louisiana flood to describe a flood transition zone for southeastern Louisiana. We show that the interaction of rainfall excess with coastal surge is nonlinear and less than the superposition of their individual components. Our analysis provides a foundation to define flooding zones across coastal landscapes throughout the world to support flood risk assessments.

**Plain Language Summary** Flooding in coastal communities can be caused by a variety of events, such as tides, hurricane storm surge, and intense rainfall. Large amounts of rain over inland regions can cause rivers, creeks, and canals to overflow their banks and flood neighboring areas. Waters around and within these rivers, creeks, and canals flow into the ocean. However, these inland water levels can interact with a high tide or surge from the ocean. This can complicate matters when rivers are draining rainwaters to the ocean, while at the same time, the ocean is pushing water inland. When these types of events occur, water levels and the resulting floodwaters in the surrounding communities are influenced by both rainfall and coastal processes. We define this region as a flood transition zone. Our analysis provides a foundation to define flooding zones across coastal landscapes to support flood risk assessments. In addition, we show that the combination of rainfall excess with coastal surge is less than the addition of their individual contributions. Identifying the transition zone for coastal communities worldwide can result in better planning and preparedness before these types of natural disasters occur, which will protect property and save lives.

### 1. Introduction

Recent storms have caused catastrophic flooding in coastal communities: the April 2016 Houston flood, 2016 Louisiana flood, Hurricane Harvey-related flooding in Texas and Louisiana (August 2017), Hurricane Irma in Florida (September 2017), and Hurricane Maria in Puerto Rico (September 2017). Such events have generated interest in the driving mechanisms and disparate flood types that occur across low-gradient coastal regions and river deltas. Flooding can emerge from extreme rainfall, coastal surges, or a combination occurring in tandem or in close succession (Hunt, 2005; Ray et al., 2011; Wahl et al., 2015; Zheng et al., 2013). Interior regions can experience pluvial and fluvial flooding whereby soils become saturated and river networks are at or have exceeded capacity. In contrast, near the coast, flooding is driven by storm surges from tropical cyclones or strong winds (e.g., cold fronts). As a result, we hypothesize that there is a transitional area where flooding can occur from compounded rainfall excess and coastal inundation (Figure 1). Conditions upland alter flooding downstream adjacent to the coast and conditions at the coast alter inundation upstream. Our goal in this paper is not to recreate or validate historic flood events but to develop a diagnostic tool to assess the potential effects and implications of compound flood events and to explore and define a flood transition zone.

The interaction between intense rainfall and coastal surges and their influence on overland flooding is multifaceted. Statistical and numerical models employed to examine such events are relatively new (Dube et al.,

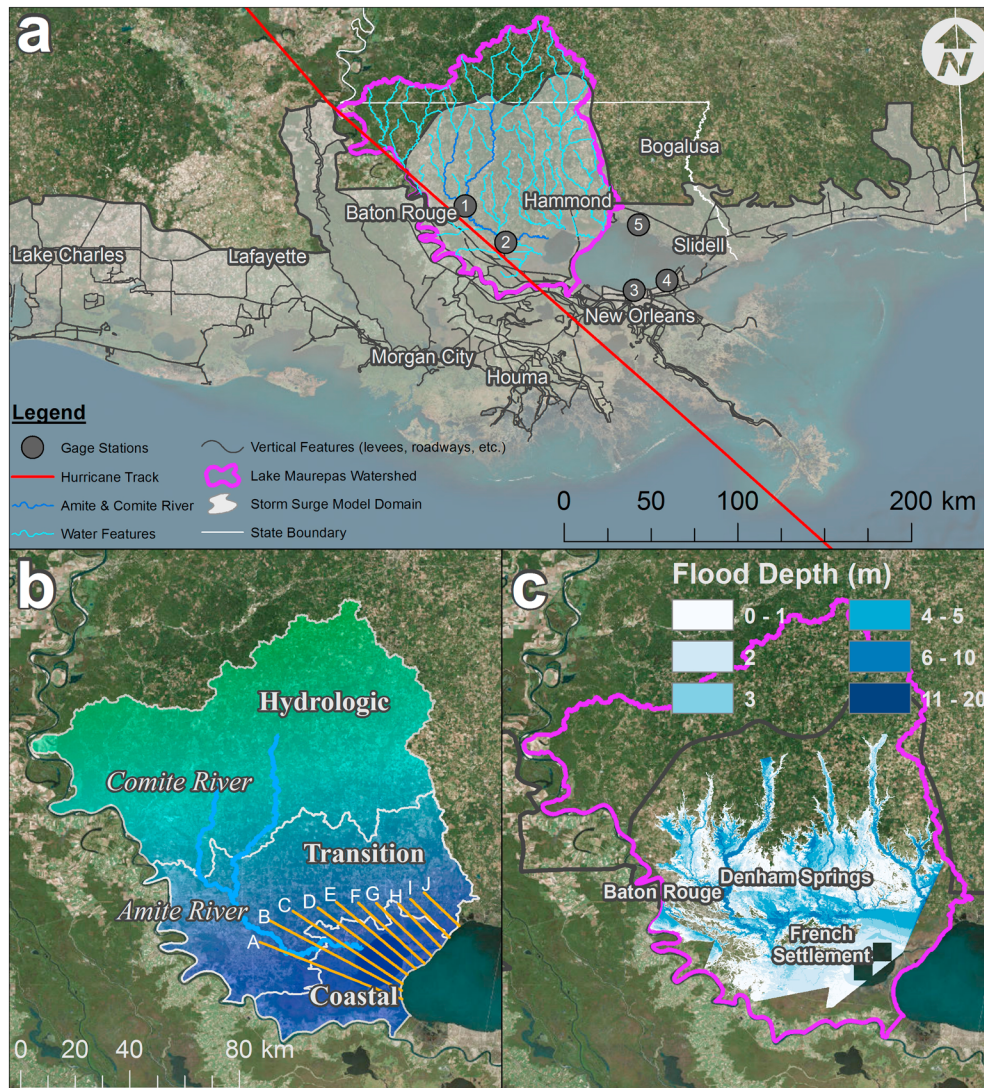


**Figure 1.** (a) Coastal Louisiana with focus on the Lake Maurepas watershed (purple polygon). The extent of the storm surge model is in the shaded gray and includes portions of the Lake Maurepas watershed. Gage stations shown are listed as (1) Amite River at Denham Springs (USGS 07378500), (2) Amite River near French Settlement (USGS 07380200), (3) New Canal Station (NOAA 08761927), and (4) USGS-DEPL\_SSS-LA-ORL-014 and USACE\_85575. (b) Zoom-in of the Lake Maurepas watershed with hypothesized regions of coastal (blue) and hydrologic (green) flooding and flooding transition zone between. The transects labeled A-J will be used to explain flood transition. (c) Inundation depth (above ground) and extent for the 2016 Louisiana rainfall event derived from FEMA (2016).

1986; Hunt, 2005). Statistical methods have demonstrated that it is necessary to consider the dependence between extreme rainfall and storm surge for flood risk assessments (Zheng et al., 2013) and that the likelihood of their joint occurrence is higher along the Gulf and east U.S. coast than the Pacific. Such events have also increased over the past century (Wahl et al., 2015). Deterministic models of storm surge and rainfall runoff have been combined in a geographic information system framework to quantify their combined hazard and exposure (Thompson & Frazier, 2014). Other numerical modeling studies have shown that the combined effects of freshwater river discharge and rainfall runoff, including their timing, increase the magnitude of inland flooding (Chen & Liu, 2014; Ray et al., 2011). The integration of hydrodynamic and hydrologic models have resulted in more accurate simulations of peak water levels, extent of inland flooding, and surge recession during tropical cyclones (Bacopoulos et al., 2016; Silva-Araya et al., 2018).

While such modeling studies have recognized that compound flood events are likely and complex, there are knowledge gaps in how to delineate regions where flooding occurs from both rainfall excess and storm surge (flood transition zone). Herein, we present a method to delineate flood transition zones, and coastal and

hydrologic flood zones. The method is applied for a coastal watershed in southeastern Louisiana, but it can be employed for any coastal or deltaic region worldwide. This effort was implemented in rapid fashion days after the August 2016 Louisiana flood event, addressing a request by local and state officials to determine the effects that a tropical system making landfall near southeastern Louisiana could have on already distressed watershed.

## 2. 2016 Louisiana Rainfall Event

On 5 August 2016 an “unnamed” subsynoptic-scale low-pressure system developed along the Florida/Alabama state line, progressed westward, and caused precipitation for three days (August 12–14, 2016) across southeastern Louisiana (Wang et al., 2016) (Figure 1a). Observed precipitation at a rain gauge east of Baton Rouge recorded rainfall of 648.3 mm over the three-day period and a National Oceanic and Atmospheric Administration (NOAA) gauge-based gridded ( $25^{\circ} \times 25^{\circ}$ ) analysis yielded a maximum rainfall of 534.77 mm (van der Wiel et al., 2017). The intense precipitation cascaded into catastrophic flooding (Burton & Demas, 2016) that resided over the landscape for several days and weeks and affected 400,000 people (see Text S1, Chen & Knutson, 2008); Text S2, Higgins et al., 2000; Figure S1, and Figure S2). According to the Baton Rouge Area Chamber of Commerce, 41.5% of homes within the Baton Rouge region flooded with an economic impact of USD 20.7 billion (Baton Rouge Area Chamber, 2016). Estimates from the Louisiana Governor’s Office of Homeland Security and Emergency Preparedness indicated that over 60,000 houses were damaged, over 109,000 people or households applied for housing assistance, and 13 people died.

On 18 August, a few days after the rainfall diminished and runoff floodwaters were still rising, the National Hurricane Center (NHC) began to monitor a tropical wave tracking westward in the Atlantic Ocean and by 24 August the NHC identified likely development into a tropical depression (Berge, 2016). As the storm system continued to move westward, state and local officials started to ask what impacts a tropical system making landfall in the Louisiana/Mississippi region might have on the saturated soil and ponded floodwaters. These were serious questions as first responders conducted search and rescue missions, supplies were transported, and shelters for evacuees were being established. What would become Hurricane Hermine turned toward the northeastern Gulf and made landfall near St. Marks, Florida.

## 3. Methods

### 3.1. Site Description

The study area is the Amite River and Lake Maurepas watershed (herein referred to as the Lake Maurepas watershed) and Lake Pontchartrain, which is the principal drainage system for metro Baton Rouge (Figure 1). The area is typical of what can be found in deltaic regions throughout the world. The watershed contains the Amite River, Comite River, and Lake Maurepas and has a total area of 12,445 km<sup>2</sup>. Elevations across the watershed range from over 100 m NAVD88 in the upper basin in southwestern Mississippi to less than 1 m NAVD88 in the wetlands surrounding Lake Maurepas (Figure S3). The Comite River is a tributary of the Amite River and joins near Denham Springs north of Interstate 12. The Amite River outflows into Lake Maurepas south of French Settlement.

Lake Maurepas has a major axis of 20 km (southwest-northeast direction), a minor axis of 14 km (southeast-northwest direction), and an average depth of 3.0 m. Lake Maurepas empties into Lake Pontchartrain through a narrow (400 m width) 10 km canal that is 12 m in depth. Lake Pontchartrain has a depth of 3.7 m, a major axis of 66 km (east-west direction), and minor axis of 40 km (north-south direction). On average, Lake Maurepas and Pontchartrain receive minimal freshwater river input and have a limited connection to the open ocean via three narrow tidal channels, which include the 15 km Rigolets tidal channel that joins the east end of Lake Pontchartrain to Lake Borgne (Figure S3b) (Li et al., 2010). Astronomic tides within Lake Pontchartrain and Maurepas are diurnal with ranges (mean high water minus mean low water) of 16 and 10 cm, respectively; however, peak water levels can be influenced by local meteorology (Chao et al., 2012; Hamilton et al., 1982; Hsu et al., 1997). Lake Maurepas is surrounded by palustrine-forested wetlands to the west and palustrine emergent wetlands to the east. Estuarine emergent wetlands surround Lake Pontchartrain to the west and east and developed regions on the south shore near New Orleans, on the southeast near Slidell, and Mandeville to the north.

### 3.2. Flood Extent and Depth Data

Flood extent and depth data for the study area were provided by the Federal Emergency Management Agency (FEMA) ArcGIS GeoPlatform for DR 4277 (FEMA, 2016). The flooding depth was created using the best available data at the time. Data included provisional high water marks (HWMs) (as of 30 August 2016) and U.S. Geological Survey and United States Army Corps of Engineers river gages pulled on 17 August 2016 to represent river crest elevations. Coarse flowpaths were generated for gaged streams, and water levels were interpolated from the peak water levels at each gage to create a triangular irregular network. A raster was created from the triangular irregular network and snapped to a 5 m digital elevation model of Louisiana (<http://atlas.lsu.edu/>) in order to create the depth grid (Figure 1c).

### 3.3. Numerical Model Description, Validation, and Experiments

Simulations were performed using a SWAN + ADCIRC hydrodynamic model of coastal Louisiana (Figure S3) (Cobell et al., 2013; Dietrich, Zijlema, et al., 2011; Luetlich & Westerink, 2000; Roberts & Cobell, 2017; Westerink et al., 1994), which spans the western north Atlantic Ocean, Caribbean Sea, and Gulf of Mexico. The model has been validated for tides and Hurricanes Katrina (2005), Rita (2005), Gustav (2008), and Ike (2008) (Bunya et al., 2010; Dietrich, Westerink, et al., 2011; Dietrich et al., 2012; Hope et al., 2013; Roberts & Cobell, 2017). Herein we focus on model validation on Hurricane Gustav. The model was forced by astronomical tides (Q1, O1, P1, K1, N2, M2, S2, and K2) obtained from the Oregon State University Tidal Database (Egbert & Erofeeva, 2002; Egbert et al., 1994) applied at the model's open ocean boundary (60° west meridian), wind and pressure fields of Gustav (Dietrich, Westerink, et al., 2011), and river flow for the Atchafalaya (1,982 m<sup>3</sup>/s) and Mississippi Rivers (4,729 m<sup>3</sup>/s) (Roberts & Cobell, 2017). For validation purposes, the Inner Harbor Navigation Canal Lake Borgne Surge Barrier and Seabrook Floodgate were altered, as they were not constructed during Gustav. Precipitation from the hurricane was not considered. Simulated water levels were in good agreement with gage measurements and surveyed HWMs (94.7% of the HWMs had an error within  $\pm 0.5$  m, and 70% of the simulated HWMs were within 20% of the measured value) (Text S3 and Figures S4–S7) (Bilskie et al., 2016).

Three synthetic numerical experiments were performed to explore the interaction of rainfall excess and storm surge inundation for the Amite River watershed: (1) rainfall excess (R), (2) hurricane storm surge (S), and (3) rainfall excess and hurricane storm surge (RS). Maximum flood depths obtained through FEMA were used to initialize simulation R (section 3.3), in addition to astronomical tidal forcing along the open ocean boundary. Simulation S was forced by a hypothetical hurricane representative of a Hurricane Gustav-like storm as well as tidal forcing along the open ocean boundary. Hurricane parameters from Gustav advisory 27 from the NHC were employed with a track shifted to the east (Figures 1a and S3a). The storm was shifted to create a larger storm surge impact east of the Mississippi River, specifically in Lake Pontchartrain and Maurepas. Simulation RS was similar to S but also included rainfall excess flooding as an initial condition. This simulation allows a dynamic interaction of the rainfall excess flooding with the tides, hurricane winds, and resulting storm surge.

## 4. Results

Time-dependent simulated water levels across southeastern Louisiana for model simulations R, S, and RS are shown in Figure 2. Initial water levels (time = 0 days) for simulation R were high (greater than 5 m) in the upper reaches of the Lake Maurepas watershed due to the initial flood depths (Figure 1c). After 1.5 days water levels began to recede and empty into Lake Maurepas and Pontchartrain with modeled water levels ranging from 1 to 2 m NAVD88 (Figure 2d). Simulated flooding after 1.75 days (Figure 2g) shows small changes in the recession of water levels in the watershed from 6 hr prior; however, water levels remained high in Lake Maurepas and Pontchartrain owing to the limited and narrow outlets to the Gulf of Mexico.

In simulation S, water levels were low in southeastern Louisiana as the hurricane center was located offshore (Figure 2b). Once the hurricane made landfall and tracked south of New Orleans, easterly winds over the watershed and Lake Maurepas caused surge heights of 2 m NAVD88 along the western shore (Figure 2e). At 1.75 days, the winds shifted to a southerly direction. This forced the storm surge to rotate clockwise within Lake Maurepas and Pontchartrain with water levels near 2.75 m NAVD88 along the north shore (Figure 2h). For the duration of the storm, simulated peak water levels for S were near 4 m NAVD88 on the western

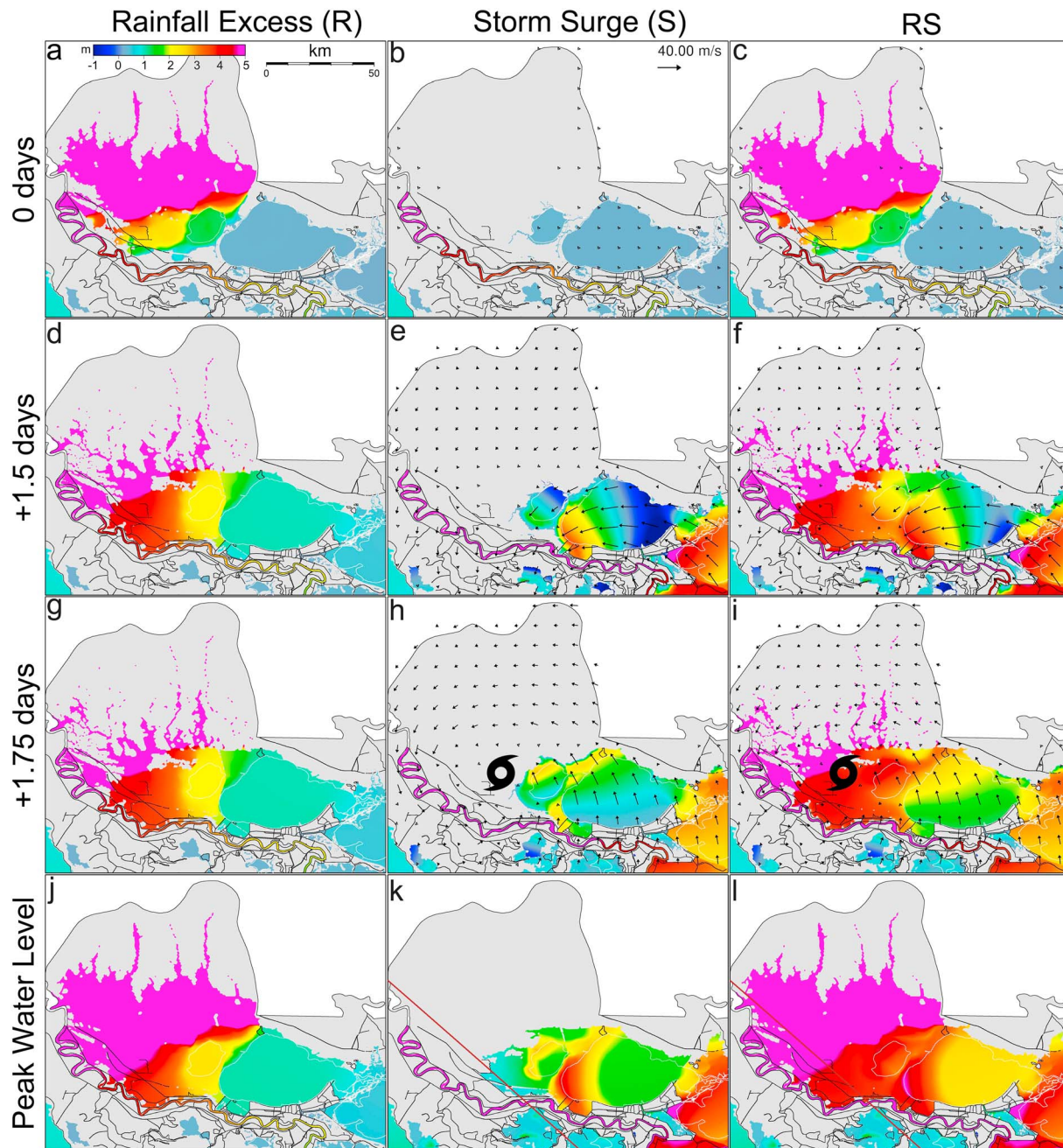


**Figure 2.** (a–c) Simulated water levels (m, NAVD88) for R (rainfall excess), S (hurricane storm surge), and R (rainfall excess and hurricane storm surge) at zero days (hurricane located well offshore and surface water flood initialized), respectively; (d–f) +1.5 days (center of hurricane is located southwest of New Orleans); (g–i) +1.75 days (center of hurricane located southeast of Baton Rouge), respectively; (j–l) simulated peak water levels (m, NAVD88) obtained for R, S, and RS, respectively, for the duration of the entire simulation period. The vectors represent wind speed (m) and direction. The black lines represent flood protection infrastructure (i.e., levees and floodwalls) and major raised roadways, and the white lines represent the shoreline.

shore of Lake Pontchartrain and over 6 m NAVD88 along the east bank of the Mississippi River levee (Figure 2k).

Water levels from simulation RS, which combine rainfall excess (R) with the hurricane storm surge (S) in a single simulation, are equal to those from R at 0 days (Figure 2c). However, as the storm approached the coast (1.5 days) and winds shifted to an easterly direction (as in S), rainfall excess propagating downstream into Lake Maurepas joined with the surge being pushed to the west bank of the Lake (Figure 2f). Six hours later (1.75 days), as the winds shifted to a southerly direction, water levels along the northern Lake Maurepas

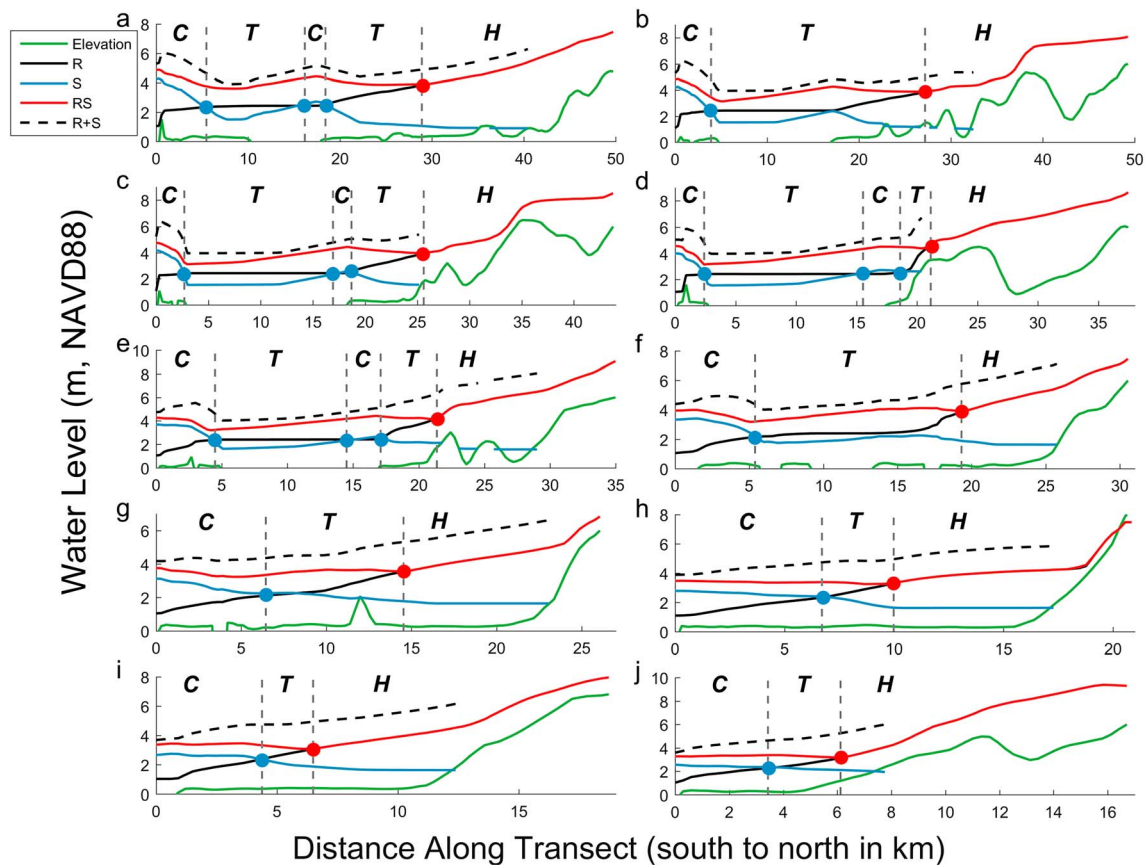


**Figure 3.** (a–j) Topographic elevations (green lines) and simulated maximum water levels (m, NAVD88) across the 10 transects shown in Figure 1b. A distance of 0 km corresponds to the Lake Pontchartrain shoreline. The black lines are results from the rainfall excess simulation (R), the blue lines are the results from the hurricane storm surge simulations (S), and the red lines are from the coupled surface water flooding and hurricane storm surge simulations (RS). Water level values for the R (black line) and RS (red line) lines are equal in the hydrologic zone. The dashed black lines are the linear addition of the individual results of R and S (R + S). The vertical dashed lines represent and the blue dots represent the change between coastal (C) and transition (T), or vice versa, and the red dots represent the change from transition (T) to hydrologic (H). Note: The difference between all R + S and RS curves demonstrates that interaction of rainfall excess with coastal surge is nonlinear and less than the linear superposition of excess and surge.

shore increased and were enhanced by 0.75 m as compared to simulation S (Figure 2i). In general, total simulated water levels within Lake Maurepas and Pontchartrain were greater in simulation RS (Figure 2l) than S (Figure 2k). The rainfall excess across the watershed increased water levels within Lake Maurepas and Pontchartrain, and the strong winds amplified water levels causing larger flood depths around the adjacent low-lying regions.

To investigate the influence and interaction of rainfall excess with storm surge, maximum water levels across 10 transects (Figure 1b) for each simulation (R, S, and RS) were analyzed (Figure 3). The transects are located across Lake Maurepas and the adjacent low-lying floodplain (Figure 1) and extend northwest starting from the northwest Lake Pontchartrain shore to the 6 m (NAVD88) contour. Peak water levels from simulation RS (combined rainfall excess and storm surge) produced a nonlinear and complex water level profile. The nonlinearity is exemplified by plotting the linear addition of rainfall excess plus hurricane storm surge (R + S) (Figure 3). The result of R + S deviates from RS (rainfall excess and storm surge in a single simulation) and has a positive bias. Therefore, adding water levels from a rainfall excess simulation to a surge simulation will likely result in a large over-prediction of water levels.

For all transects, peak water levels were greater in simulation S than R along the Lake Pontchartrain shore (transect distance of 0 km). In contrast, maximum water levels were larger (greater than 6 m NAVD88) in simulation R than S at the furthest extent of each transect. As with simulation S, water levels in simulation RS were high near the coast; however, water levels were larger than those computed in R along the coast and in the adjacent floodplain until water levels were equal to between R and RS. This is the location at which hydrologic

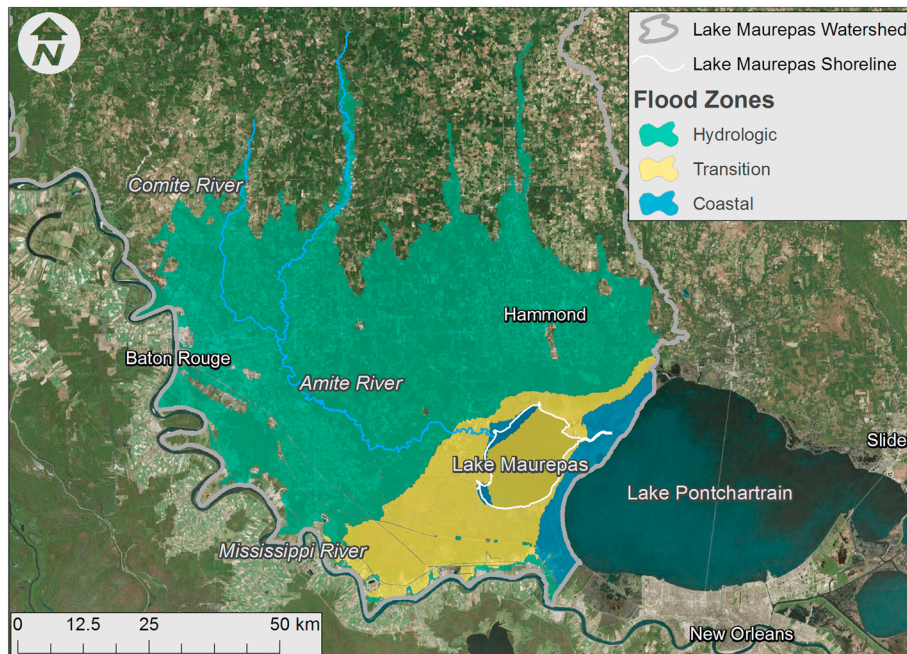


**Figure 4.** Flood zones in the Lake Maurepas watershed resulting from the 2016 Louisiana flood followed by a Hurricane Gustav-like storm. The Lake Maurepas shoreline is shown in white.

flooding is dominant and coastal surge does not have an impact on total water levels. Similarly, from the shoreline to the north, water levels from coastal flooding (S) were larger than the rainfall-induced flooding (R) until they intersect. These locations were near inflection points in the water level profile of simulation S, in particular when the water levels from S were larger than R. Therefore, a transitional region occurs where water levels from simulation S are less than R; this is where hydrologic and coastal flooding interact, and neither are dominant.

In some areas, such as in Transect A, C, D, and E (Figure 3), more than one coastal and transition zone was defined. These locations are near the northern shoreline of Lake Maurepas (distance of 16 and 18 km for Transect A). Two coastal and transition zones are present because of the small landmass between Lake Pontchartrain and Maurepas. The landmass is not inundated with rainfall excess but inundated from coastal surge with strong northerly and southerly winds.

Analyzing peak water levels across each transect provides a basis to define individual flooding zones, such as coastal (C), hydrologic (H), and transition (T). In general, the coastal zone is the region where peak water levels from storm surge inundation (S) are greater than rainfall excess (R). For the hydrologic zone, the water levels from rainfall excess are equal to the simulation including rainfall excess and storm surge (RS). Between the coastal and hydrologic regions is the transition zone. Intersection points occur where storm surge water levels equal rainfall excess (blue points) and where rainfall excess equals rainfall excess plus storm surge (red points) (Figure 3). For a given rainfall and coastal surge scenario, each of the three regions (coastal, hydrologic, and transition) can be delineated. Therefore, the transition zone is defined as  $\eta_R > \eta_S$  and  $\eta_{RS} > \eta_R$  where  $\eta$  is the maximum simulated water level. The coastal zone is defined as  $\eta_S > \eta_R$  and the hydrologic zone as  $\eta_R > \eta_S$ .

Using the definitions above, the spatial extent of the coastal, transition, and hydrologic zones within the Lake Maurepas watershed were identified (Figure 4). The narrow coastal region begins along the northeast Lake Pontchartrain shore and meets the transition zone near the eastern shoreline of Lake Maurepas. In general, most of Lake Maurepas is within the transition zone, where both coastal flooding and hydrologic flooding influence total water levels; however, there are two small areas identified as coastal zones. The transition zone is narrow to the east and widens along the southeastern portion of the watershed. North of Lake Maurepas, the hydrologic flooding zone governs and continues upland and spans the majority of the remaining watershed. These zones follow similar patterns as the hypothesized regions shown in Figure 1b.

## 5. Discussion and Conclusion

Model results across the 10 transects demonstrate the variability of peak water levels for each of the numerical experiments and the addition of individual components of rainfall excess and surge (Figure 3). The novel finding of the nonlinear interaction of surge and rainfall excess demonstrates that linearly combining the discrete mechanisms lead to an over-estimation of peak water levels and therefore flood risk, which is common practice (Thompson & Frazier, 2014). In fact, the largest divergences were shown in the maximum extent of surge inundation.

The nonlinearity of rainfall excess and surge emerges from uniting their individual, governing processes under the coupled simulation. Rainfall excess is gravity-driven flow, while surge is wind-driven and can oppose gravity-driven flow at high wind speeds. In the coupled simulation (RS), rainfall excess is exposed to the local wind in Lake Maurepas and Pontchartrain. Similarly, water levels within the lakes were exposed to upstream conditions of rainfall excess. These additional forcing mechanisms nonlinearly alter the response of water levels. The region where both surge and rainfall excess provide a major contribution to the peak water levels was defined as the transition zone. In the upland reaches, hydrology dominates flooding and surge does not contribute to additional inundation. Likewise, near the coast, there is also an increase in water level from rainfall excess, but surge is the dominant mechanism contributing to peak water levels. This highlights the importance of accounting for the effects of both rainfall excess and coastal surge.

This work demonstrates how coupled coastal inundation and hydrologic rainfall runoff models can be employed to define flood transition zones. The delineated coastal, transition, and hydrologic flood zones (Figure 4) show the spatial variability and influence of a coupled rainfall and storm surge scenario. However, it is important to note that the delineated flood zones are likely to change for varying scenarios and intensities of precipitation and coastal surge (i.e., wind-driven) events, as well as their relative timing (Ray et al., 2011). For example, less intense rainfall may allow storm surge to dominate further upland or more intense rainfall may allow rainfall excess to dominate further downstream. Such circumstances are likely to occur during a tropical cyclone event that delivers storm surges and intense precipitation during a short time period. Future efforts will focus on delineating flood zones based on a suite of events with varying magnitudes and relative timing.

Meteorological studies performed after the 2016 Louisiana flood event indicate that this type of low probability, nonhurricane-related event is not unusual for Louisiana and may become more common and intense (van der Wiel et al., 2017) and around the world (Gordon et al., 1992; Kendon et al., 2014). In addition, tropical systems themselves can bring about extreme precipitation and large storm surges. This was the case with Hurricane Harvey, which brought devastating storm surges to the south Texas coast and over 1,000 mm of rainfall to the Houston area (Blake & Zelinsky, 2017). Hurricane Irma delivered intense rainfall (over 400 mm) across the Florida peninsula and areas along the western coast experienced several hours of low water levels prior to the maximum surge. This drained numerous back bays (e.g., Tampa Bay) and waterways along the coast and created a complex interaction of coastal and overland hydrologic processes (Cappucci, 2017). Across Puerto Rico, Hurricane Maria produced over 760 mm of rain and up to 3 m of storm surge. These types of coastal flood events can affect the livelihood of resource-rich coastal communities (Rueda et al., 2017) and point to the need to consider the combined effects of rainfall excess and storm surge (Wahl et al., 2015).

Delineating flood transition zones has a variety of implications and can provide influential information for coastal scientists, resource managers, and stakeholders within coastal watersheds worldwide. First, from a numerical modeling perspective, the transition zone can inform where there should be overlap and communication among hydrologic and coastal models. From a risk-based perspective, the defined transition zones provide coastal communities with a detailed perspective of perceived flood vulnerability for a given region. Within the transition zone, the impact of disparate events may be minor, but a particular combination may lead to an extreme scenario (Leonard et al., 2014; Wahl et al., 2015). From a hydrologic and biologic perspective, the transition zone may be a proxy for the vulnerability of saltwater intrusion or environmental stressors related to coastal inundation (McKee & Mendelsohn, 1989; Nicholls & Cazenave, 2010; Pezeshki et al., 1990). From a coastal management perspective, the presented modeling methods can be used to consider potential engineered or natural and nature-based features to determine their relative effectiveness of reducing risk at the regional or local scale (Bridges et al., 2015). From a community planning perspective (Adger et al.,

2005), the effects of climate change, such as sea level rise, changes in storm patterns and frequency, wetland loss, and land use change, will alter the defined flood zones.

#### Acknowledgments

The authors thank D. L. Passeri and M. R. Foster-Martinez for their helpful suggestions in editing the manuscript. This research was funded primarily from award EAR1660502 from the National Science Foundation (NSF) and in part by the Louisiana Sea Grant Laborde Chair. Simulations were performed using the High Performance Computing at Louisiana State University (LSU) and the Louisiana Optical Network Initiative (LONI). Measured rainfall extent and depth for the 2016 Louisiana flood were obtained from FEMA's Geoplatform DR4277 (<http://fema.maps.arcgis.com/apps/MapJournal/index.html?appid=efb5b1121e344e919784a2386c90ea01>). Water level data were obtained from NOAA Tides and Currents (<https://tide-sandcurrents.noaa.gov/>) and the Louisiana Coastwide Reference Monitoring System (CRMS) (<https://www.lacoast.gov/crms2/>). Model results, as shown in Figure 2, are available on FigShare (<https://dx.doi.org/10.6084/m9.figshare.5886955>). Transect data, as shown in Figure 1, are available on FigShare (<https://dx.doi.org/10.6084/m9.figshare.5880901>). The statements and conclusions are those of the authors and do not reflect the views of NSF, Louisiana Sea Grant, LSU, LONI, FEMA, or NOAA.

#### References

- Adger, W. N., Hughes, T. P., Folke, C., Carpenter, S. R., & Rockström, J. (2005). Social-ecological resilience to coastal disasters. *Science*, 309(5737), 1036–1039. <https://doi.org/10.1126/science.1112122>
- Bacopoulos, P., Tang, Y., & Hagen, S. C. (2016). Integrated hydrologic-hydrodynamic modeling of flooding in the Lower St. Johns River Basin caused by Tropical Storm Fay (2008). *ASCE Journal of Hydrologic Engineering*, 22(8). [https://doi.org/10.1061/\(ASCE\)HE.1943-5584.0001539](https://doi.org/10.1061/(ASCE)HE.1943-5584.0001539)
- Baton Rouge Area Chamber (2016). Louisiana flood 2016, Update 1, edited, Baton Rouge, LA.
- Berge, R. (2016). Hurricane Hermine, Rep., National Hurricane Center.
- Bilskie, M. V., Hagen, S. C., Medeiros, S. C., Cox, A. T., Salisbury, M., & Coggin, D. (2016). Data and numerical analysis of astronomic tides, wind-waves, and hurricane storm surge along the northern Gulf of Mexico. *Journal of Geophysical Research: Oceans*, 121, 3625–3658. <https://doi.org/10.1002/2015JC011400>
- Blake, E. S., & Zelinsky, D. A. (2017). National Hurricane Center Tropical Cyclone Report - Hurricane Harvey (pp. 1–43). Retrieved from [https://www.nhc.noaa.gov/data/tcr/AL092017\\_Harvey.pdf](https://www.nhc.noaa.gov/data/tcr/AL092017_Harvey.pdf)
- Bridges, T. S., Burks-Copes K. A., Bates M. E., Collier Z. A., Fischel J. C., Piercy C. D. et al. (2015). Use of natural and nature-based features (NNBF) for coastal resilience, Rep., U.S. Army Corps of Engineers, Alexandria, VA.
- Bunya, S., Dietrich, J. C., Westerink, J. J., Ebersole, B. A., Smith, J. M., Atkinson, J. H., et al. (2010). A high-resolution coupled riverine flow, tide, wind, wind wave, and storm surge model for southeastern Louisiana and Mississippi. Part I: Model development and validation. *Monthly Weather Review*, 138(2), 345–377. <https://doi.org/10.1175/2009MWR2906.1>
- Burton, J., & Demas, A. (2016). *Backwater flooding in Baton Rouge*. Reston, VA: USGS.
- Cappucci, M. (2017). Hurricane Irma drained the water from Florida's largest bays—But it wasn't gone for long. The Washington Post.
- Chao, X., Jia, Y., Wang, S. S. Y., & Hossain, A. K. M. A. (2012). Numerical modeling of surface flow and transport phenomena with applications to Lake Pontchartrain. *Lake and Reservoir Management*, 28(1), 31–45. <https://doi.org/10.1080/07438141.2011.639481>
- Chen, C.-T., & Knutson, T. (2008). On the verification and comparison of extreme rainfall indices from climate models. *Journal of Climate*, 21(7), 1605–1621. <https://doi.org/10.1175/2007JCLI494.1>
- Chen, W.-B., & Liu, W.-C. (2014). Modeling flood inundation induced by river flow and storm surges over a River Basin. *Water*, 6(12), 3182–3199. <https://doi.org/10.3390/w6103182>
- Cobell, Z., Zhao, H., Roberts, H. J., Clark, F. R., & Zou, S. (2013). Surge and wave modeling for the Louisiana 2012 coastal master plan. *Journal of Coastal Research*, 67, 88–108. [https://doi.org/10.2112/SL\\_67\\_7](https://doi.org/10.2112/SL_67_7)
- Dietrich, J. C., Zijlema, M., Westerink, J. J., Holthuijsen, L. H., Dawson, C. N., Luettich, R. A., et al. (2011). Modeling hurricane waves and storm surge using integrally-coupled, scalable computations. *Coastal Engineering*, 58, 45–65. <https://doi.org/10.1016/j.coastaleng.2010.08.001>
- Dietrich, J. C., Westerink, J. J., Kennedy, A. B., Smith, J. M., Jensen, R. E., Zijlema, M., et al. (2011). Hurricane Gustav (2008) waves and storm surge: Hindcast, synoptic analysis, and validation in southern Louisiana. *Monthly Weather Review*, 139(8), 2488–2522. <https://doi.org/10.1175/2011MWR3611.1>
- Dietrich, J. C., Tanaka, S., Westerink, J. J., Dawson, C. N., Luettich, R. A., Zijlema, M., et al. (2012). Performance of the unstructured-mesh, SWAN +ADCIRC model in computing hurricane waves and surge. *Journal of Scientific Computing*, 52(2), 468–497. <https://doi.org/10.1007/s10915-011-9555-6>
- Dube, S. K., Sinha, P. C., & Roy, G. D. (1986). Numerical simulation of storm surges in Bangladesh using a bay-river coupled model. *Coastal Engineering*, 10(1), 85–101. [https://doi.org/10.1016/0378-3839\(86\)90040-2](https://doi.org/10.1016/0378-3839(86)90040-2)
- Egbert, G. D., & Erofeeva, S. Y. (2002). Efficient inverse modeling of barotropic ocean tides. *Journal of Atmospheric and Oceanic Technology*, 19(2), 183–204. [https://doi.org/10.1175/1520-0426\(2002\)019%3C0183:EIMOBO%3E2.0.CO;2](https://doi.org/10.1175/1520-0426(2002)019%3C0183:EIMOBO%3E2.0.CO;2)
- Egbert, G. D., Bennett, A. F., & Foreman, M. G. G. (1994). TOPEX/POSEIDON tides estimated using a global inverse model. *Journal of Geophysical Research*, 99(C12), 24821–24852. <https://doi.org/10.1029/94JC01894>
- FEMA (2016). DR 4277 and Baton Rouge area flooding.
- Gordon, H. B., Whetton, P. H., Pittock, A. B., Fowler, A. M., & Haylock, M. R. (1992). Simulated changes in daily rainfall intensity due to the enhanced greenhouse effect: Implications for extreme rainfall events. *Climate Dynamics*, 8(2), 83–102. <https://doi.org/10.1007/bf00209165>
- Hamilton, G. D., Soileau, C. W., & Stroud, A. (1982). Numerical modeling study of Lake Pontchartrain. *Journal of the Waterway, Port, Coastal and Ocean Division*, 108(1), 49–64.
- Higgins, R. W., Shi, W., Yarosh, E., & Joyce, R. (2000). Improved United States precipitation quality control system and analysis, Rep., NOAA, National Weather Service, National Centers for Environmental Prediction, Climate Prediction Center, Camp Springs, MD.
- Hope, M. E., Westerink, J. J., Kennedy, A. B., Kerr, P. C., Dietrich, J. C., Dawson, C., et al. (2013). Hindcast and validation of Hurricane Ike (2008) waves, forerunner, and storm surge. *Journal of Geophysical Research: Oceans*, 118(9), 4424–4460. <https://doi.org/10.1002/jgrc.20314>
- Hsu, S. A., Grymes, J. M. I., & Yan, Z. (1997). A simplified hydrodynamic formula for estimating the wind-driven flooding in the Lake Pontchartrain-Amite River Basin. *National Weather Digest*, 21(4), 18–22.
- Hunt, J. C. R. (2005). Inland and coastal flooding: Developments in prediction and prevention. *Philosophical Transactions of the Royal Society A: Mathematical, Physical and Engineering Sciences*, 363(1831), 1475–1491. <https://doi.org/10.1098/rsta.2005.1580>
- Kendon, E. J., Roberts, N. M., Fowler, H. J., Roberts, M. J., Chan, S. C., & Senior, C. A. (2014). Heavier summer downpours with climate change revealed by weather forecast resolution model. *Nature Climate Change*, 4(7), 570–576. <https://doi.org/10.1038/nclimate2258>, <https://www.nature.com/articles/nclimate2258#supplementary-information>
- Leonard, M., Westra, S., Phatak, A., Lambert, M., van den Hurk, B., McInnes, K., et al. (2014). A compound event framework for understanding extreme impacts. *Wiley Interdisciplinary Reviews: Climate Change*, 5(1), 113–128. <https://doi.org/10.1002/wcc.252>
- Li, C., Weeks, E., & Blanchard, B. W. (2010). Storm surge induced flux through multiple tidal passes of Lake Pontchartrain estuary during Hurricanes Gustav and Ike. *Estuarine, Coastal and Shelf Science*, 87(4), 517–525. <https://doi.org/10.1016/j.ecss.2010.02.003>
- Luettich, R. A., & Westerink, H. J. (2000). ADCIRC: A (Parallel) advanced circulation model for oceanic, coastal, and estuarine waters, Rep. (115 pp.).
- McKee, K. L., & Mendelssohn, I. A. (1989). Response of a freshwater marsh plant community to increased salinity and increased water level. *Aquatic Botany*, 34(4), 301–316. [https://doi.org/10.1016/0304-3770\(89\)90074-0](https://doi.org/10.1016/0304-3770(89)90074-0)
- Nicholls, R. J., & Cazenave, A. (2010). Sea-level rise and its impact on coastal zones. *Science*, 328(5985), 1517–1520. <https://doi.org/10.1126/science.1185782>

- Pezeshki, S. R., Delaune, R. D., & Patrick, W. H. (1990). Flooding and saltwater intrusion: Potential effects on survival and productivity of wetland forests along the U.S. Gulf Coast. *Forest Ecology and Management*, 33–34(Supplement C), 287–301. [https://doi.org/10.1016/0378-1127\(90\)90199-L](https://doi.org/10.1016/0378-1127(90)90199-L)
- Ray, T., Stepinski, E., Sebastian, A., & Bedient, P. B. (2011). Dynamic modeling of storm surge and inland flooding in a Texas coastal floodplain. *Journal of Hydraulic Engineering*, 137(10), 1103–1110. [https://doi.org/10.1061/\(ASCE\)HY.1943-7900.0000398](https://doi.org/10.1061/(ASCE)HY.1943-7900.0000398)
- Roberts, H., & Cobell, Z. (2017). *2017 coastal master plan: Attachment C3-25.1: Storm surge, Rep* (pp. 1–110). Baton Rouge, LA: Louisiana: Coastal protection and restoration authority.
- Rueda, A., Vitousek, S., Camus, P., Tomás, A., Espejo, A., Losada, I. J., et al. (2017). A global classification of coastal flood hazard climates associated with large-scale oceanographic forcing. *Scientific Reports*, 7(1), 5038. <https://doi.org/10.1038/s41598-017-05090-w>
- Silva-Araya, W., Santiago-Collazo, F., Gonzalez-Lopez, J., & Maldonado-Maldonado, J. (2018). Dynamic modeling of surface runoff and storm surge during hurricane and tropical storm events. *Hydrology*, 5(1), 13. <https://doi.org/10.3390/hydrology5010013>
- Thompson, C. M., & Frazier, T. G. (2014). Deterministic and probabilistic flood modeling for contemporary and future coastal and inland precipitation inundation. *Applied Geography*, 50, 1–14. <https://doi.org/10.1016/j.apgeog.2014.01.013>
- van der Wiel, K., Kapnick, S. B., van Oldenborgh, G. J., Whan, K., Sjoukje, P., Vecchi, G. A., et al. (2017). Rapid attribution of the August 2016 flood-inducing extreme precipitation in south Louisiana to climate change. *Hydrology and Earth System Sciences*, 21(2), 897–921. <https://doi.org/10.5194/hess-21-897-2017>
- Wahl, T., Jain, S., Bender, J., Meyers, S. D., & Luther, M. E. (2015). Increasing risk of compound flooding from storm surge and rainfall for major US cities. *Nature Climate Change*, 5(12), 1093–1097. <https://doi.org/10.1038/nclimate2736> <https://www.nature.com/articles/nclimate2736#supplementary-information>
- Wang, S. Y. S., Zhao, L., & Gillies, R. R. (2016). Synoptic and quantitative attributions of the extreme precipitation leading to the August 2016 Louisiana flood. *Geophysical Research Letters*, 43, 11,805–811,814. <https://doi.org/10.1002/2016GL071460>
- Westerink, J. J., Blain, C. A., Luettich, R. A., & Scheffner, N. W. (1994). *ADCIRC: An advanced three-dimensional circulation model for shelves, coasts, and estuaries: Report 2, Rep* (p. 168). Vicksburg, MS: U.S. Army Corps of Engineers.
- Zheng, F., Westra, S., & Sisson, S. A. (2013). Quantifying the dependence between extreme rainfall and storm surge in the coastal zone. *Journal of Hydrology*, 505, 172–187. <https://doi.org/10.1016/j.jhydrol.2013.09.054>